



JOURNAL OF  
SYNCHROTRON  
RADIATION

**Volume 26 (2019)**

**Supporting information for article:**

**A kinetic and mechanistic study into the transformation of calcium sulfate hemihydrate to dihydrate**

**Sebastian J. Gurgul, Gareth R. Williams and Gabriel Seng**

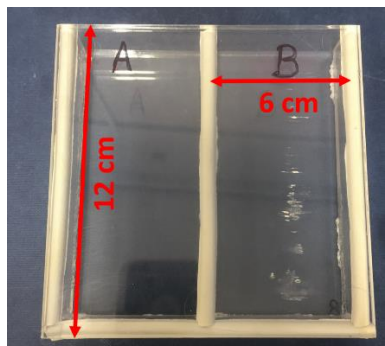


**Figure S1** The design of the in-house rig used for *in situ* diffraction studies. The depth is 1 cm.

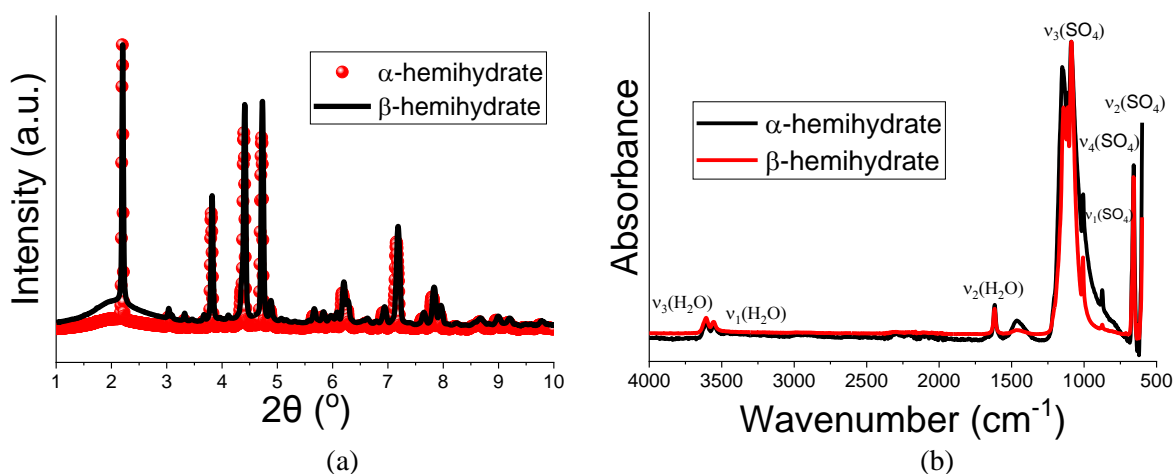


**Figure S2** (a) XRD and (b) IR data for  $\alpha$ - and  $\beta$ - $\text{CaSO}_4 \cdot 0.5\text{H}_2\text{O}$ .

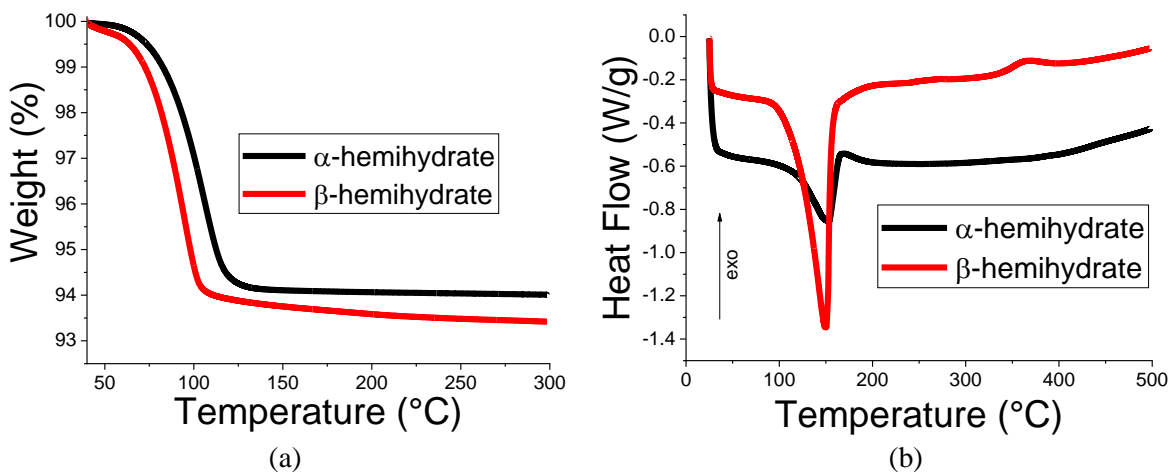


**Figure S3** (a) TGA and (b) DSC data for  $\alpha$ - and  $\beta$ - $\text{CaSO}_4 \cdot 0.5\text{H}_2\text{O}$ .

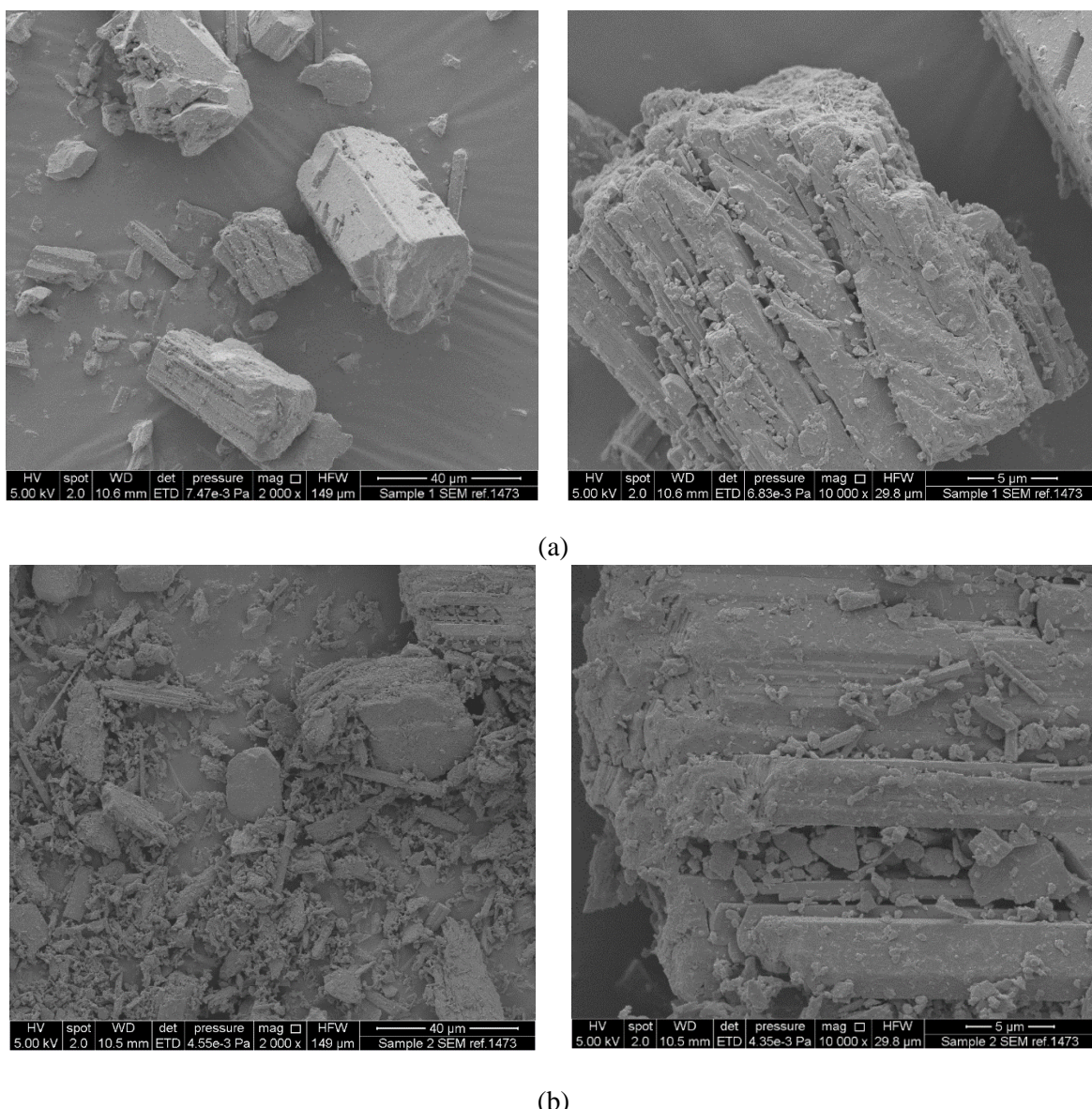


**Figure S4** SEM images of (a)  $\alpha$ - and (b)  $\beta\text{-CaSO}_4\cdot0.5\text{H}_2\text{O}$ .

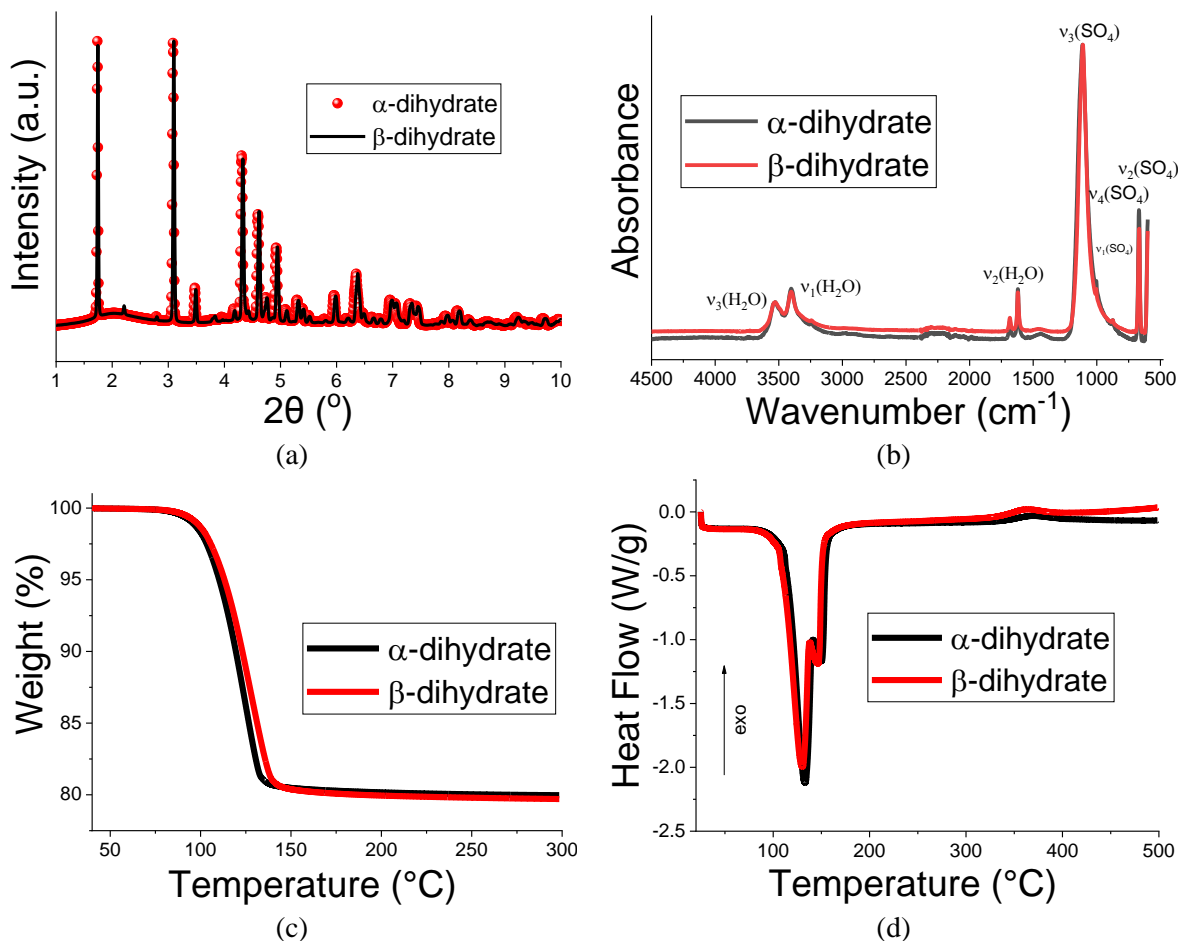


**Figure S5** Data for dihydrates obtained from  $\alpha$ - and  $\beta$ - $\text{CaSO}_4 \cdot 0.5\text{H}_2\text{O}$ . (a) XRD; (b) IR; (c) TGA; and, (d) DSC data are presented.

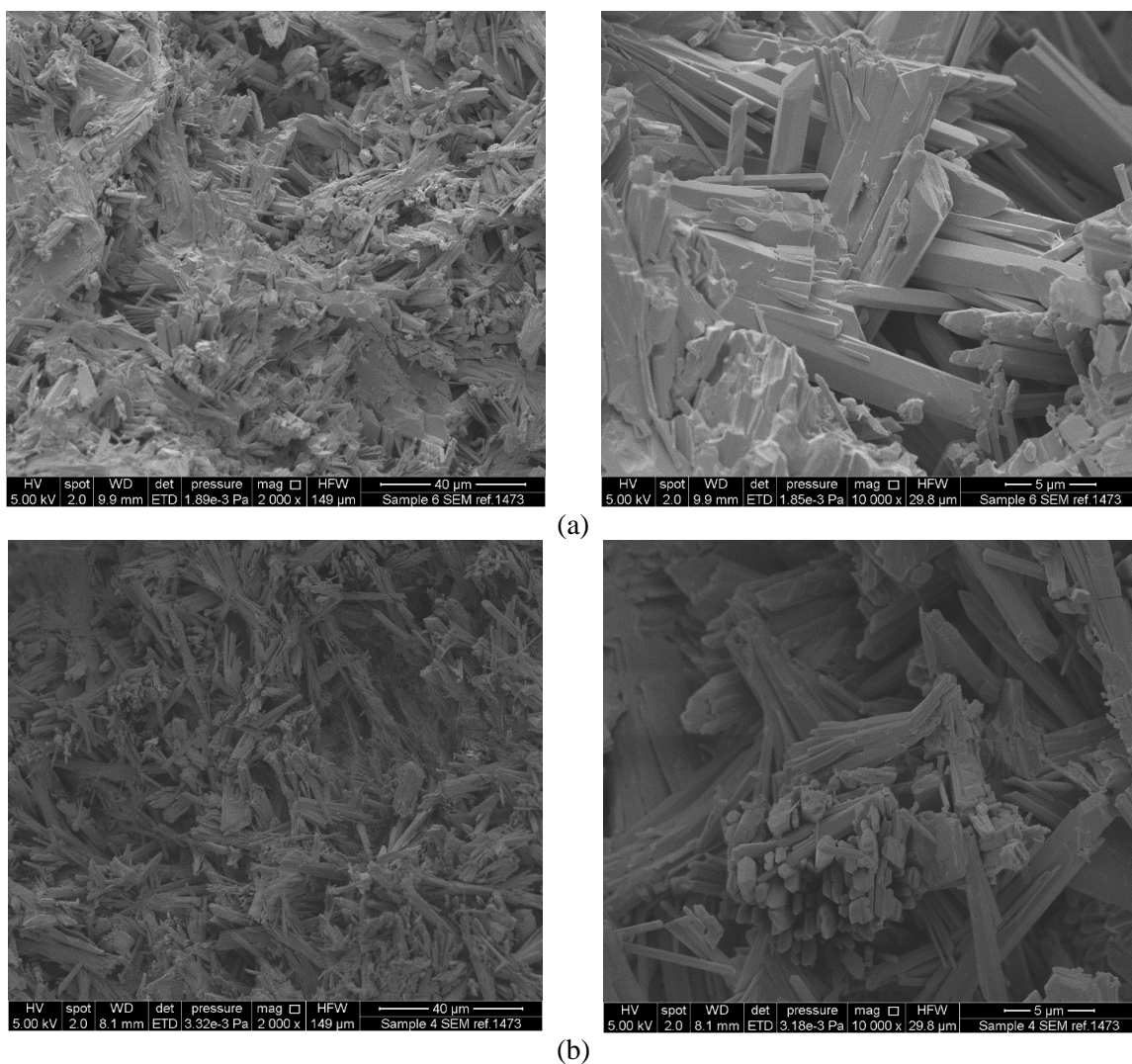


**Figure S6** SEM images of (a)  $\alpha$ - and (b)  $\beta$ -CaSO<sub>4</sub>·2H<sub>2</sub>O.

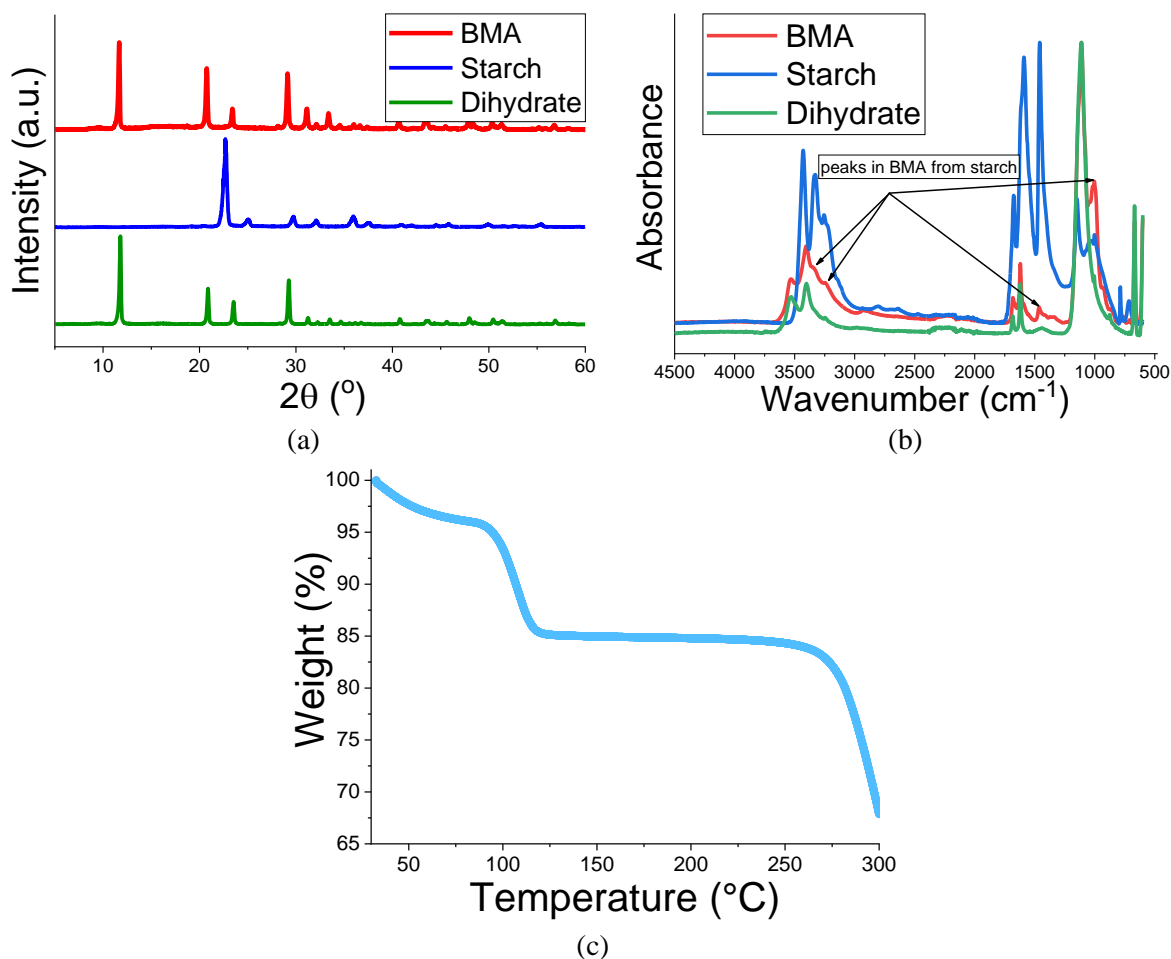


**Figure S7** (a) XRD; (b) IR; and, (c) TGA data for BMA.

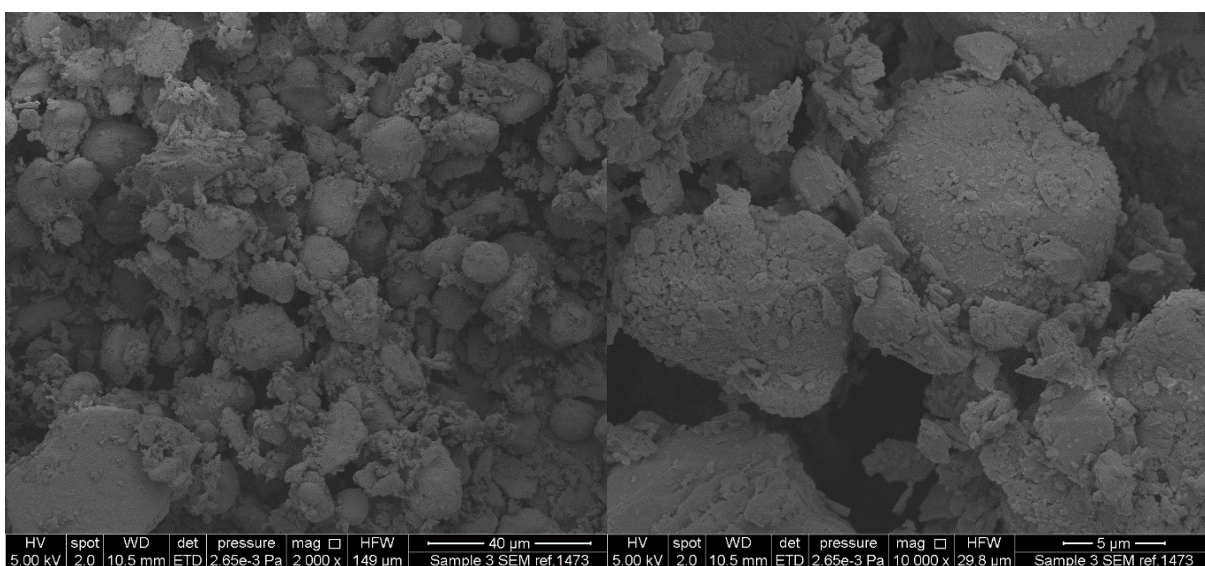


**Figure S8** SEM images of BMA.

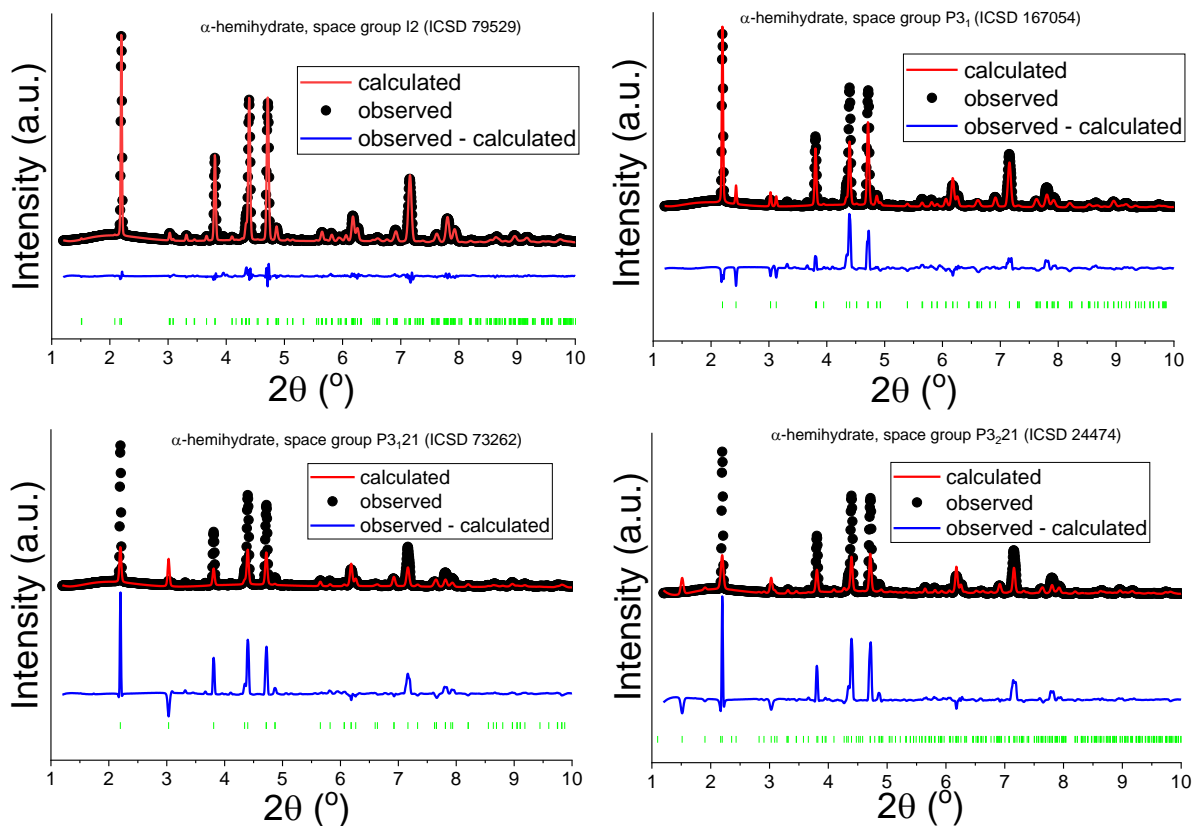


**Figure S9** The results of structural refinements with the different models reported in the ICSD for  $\alpha\text{-CaSO}_4 \cdot 0.5\text{H}_2\text{O}$ .

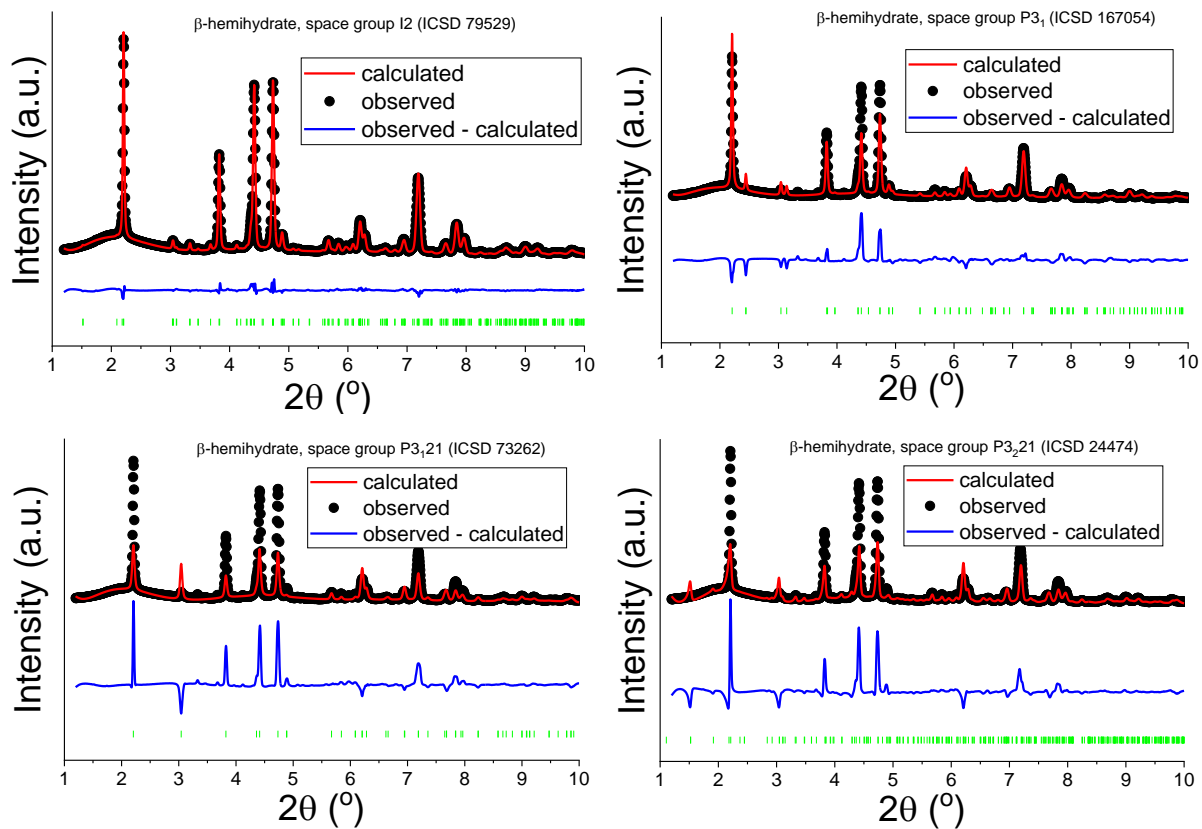


**Figure S10** The results of structural refinements with the different models reported in the ICSD for  $\beta\text{-CaSO}_4\cdot0.5\text{H}_2\text{O}$ .

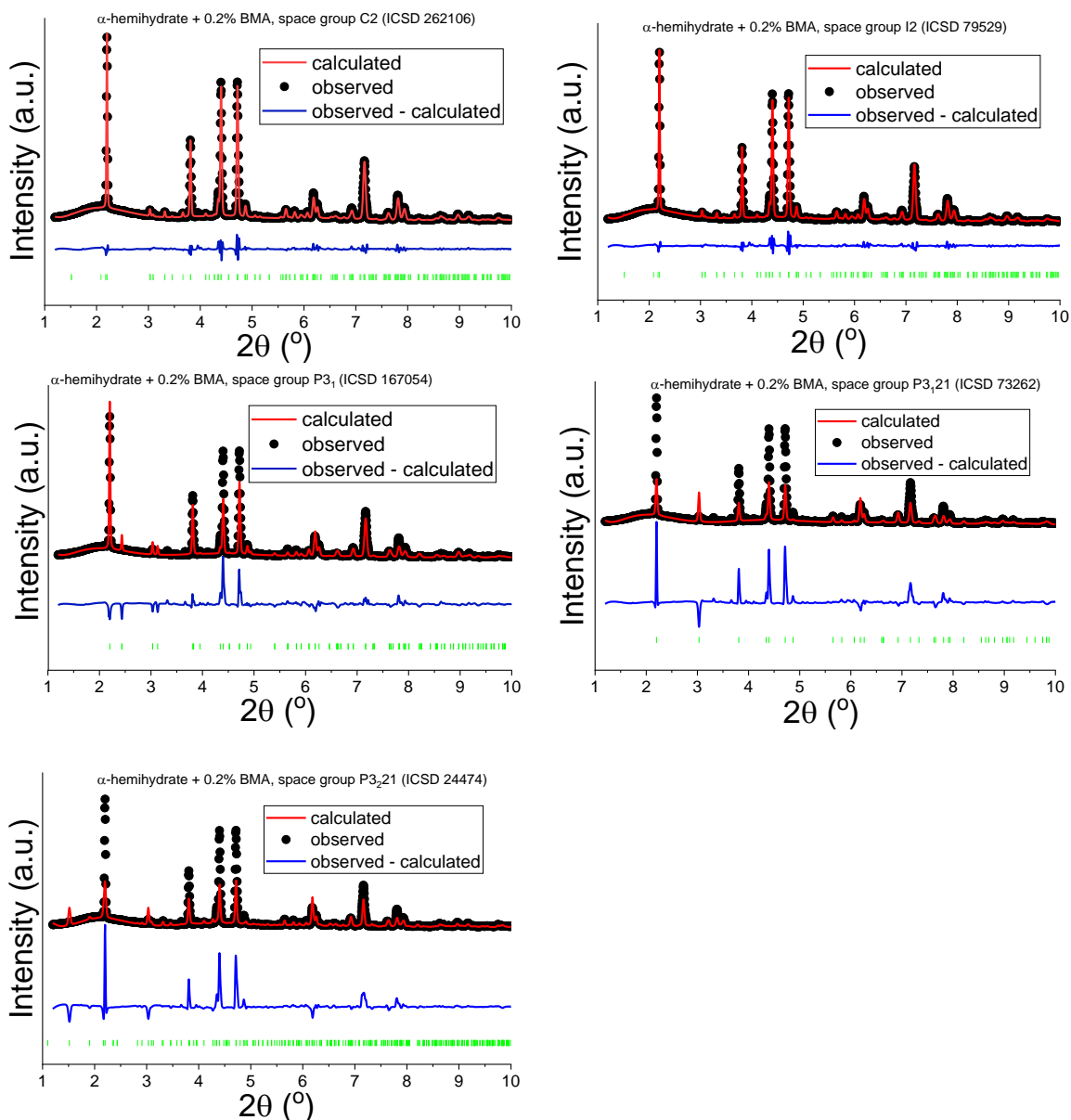


**Figure S11** The results of structural refinements with the different models reported in the ICSD for  $\alpha\text{-CaSO}_4\cdot 0.5\text{H}_2\text{O}$  with 0.2 % w/w BMA.

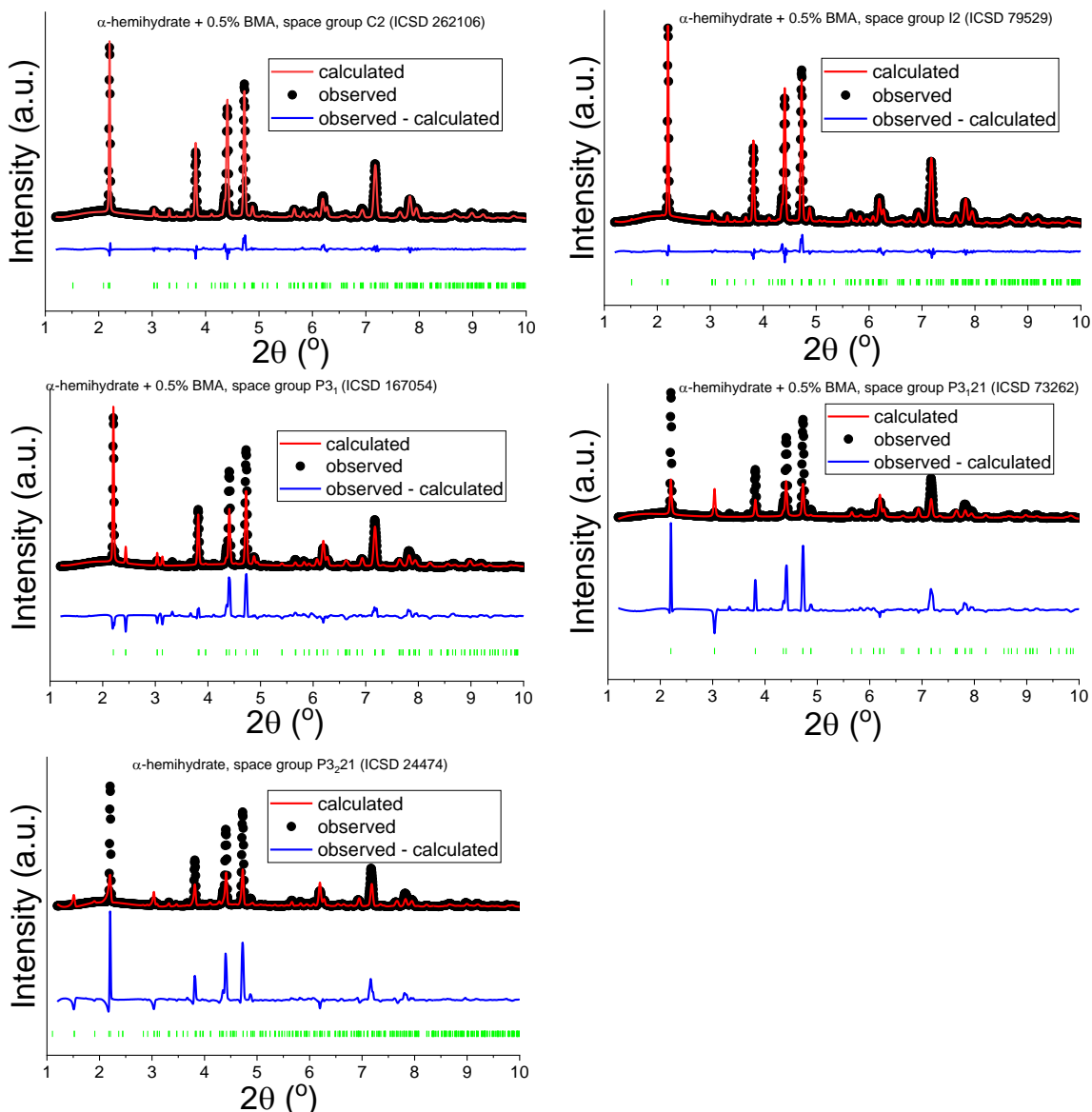


**Figure S12** The results of structural refinements with the different models reported in the ICSD for  $\alpha\text{-CaSO}_4\cdot 0.5\text{H}_2\text{O}$  with 0.5 % w/w BMA.

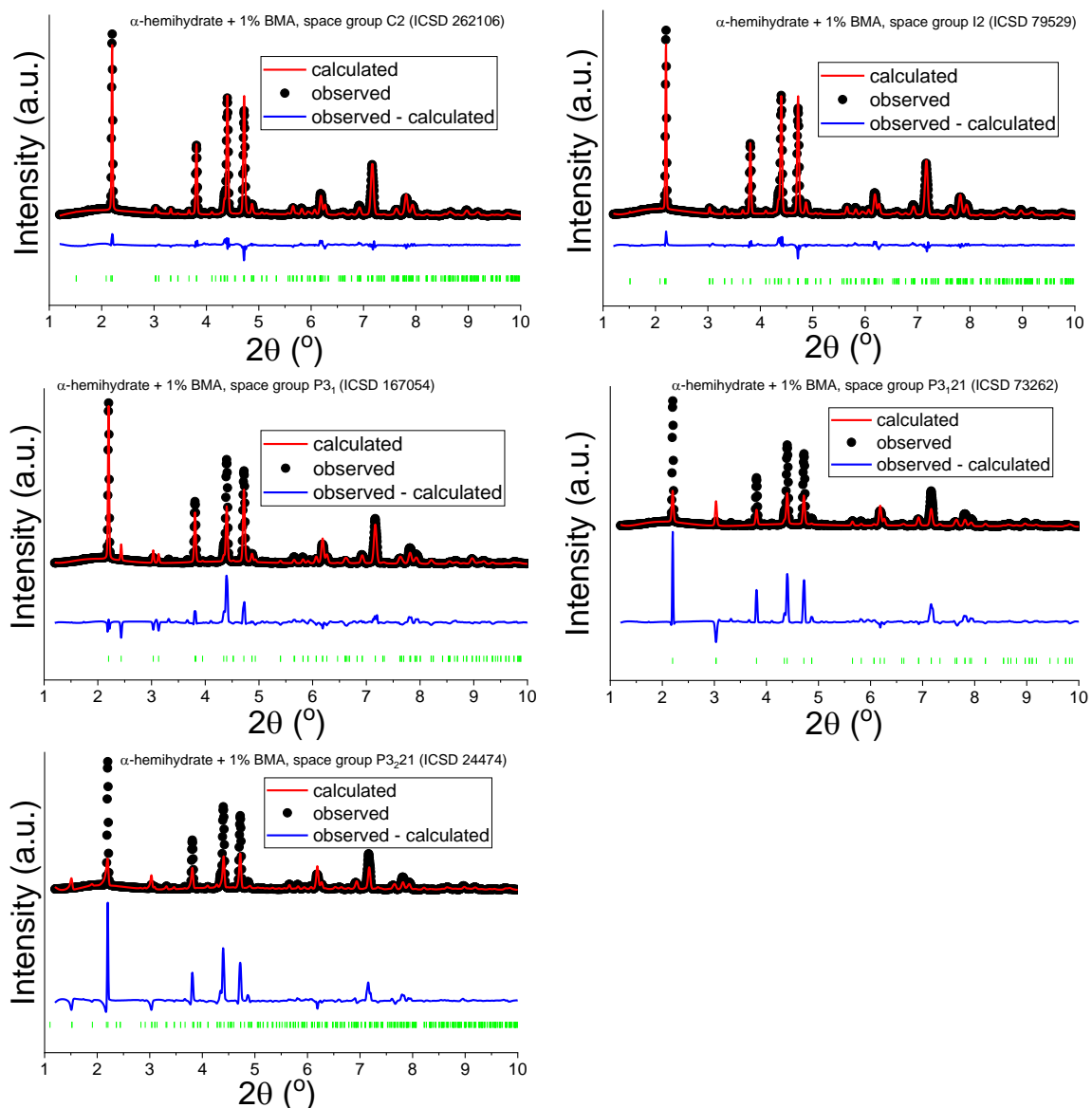


**Figure S13** The results of structural refinements with the different models reported in the ICSD for  $\alpha\text{-CaSO}_4 \cdot 0.5\text{H}_2\text{O}$  with 1 % w/w BMA.

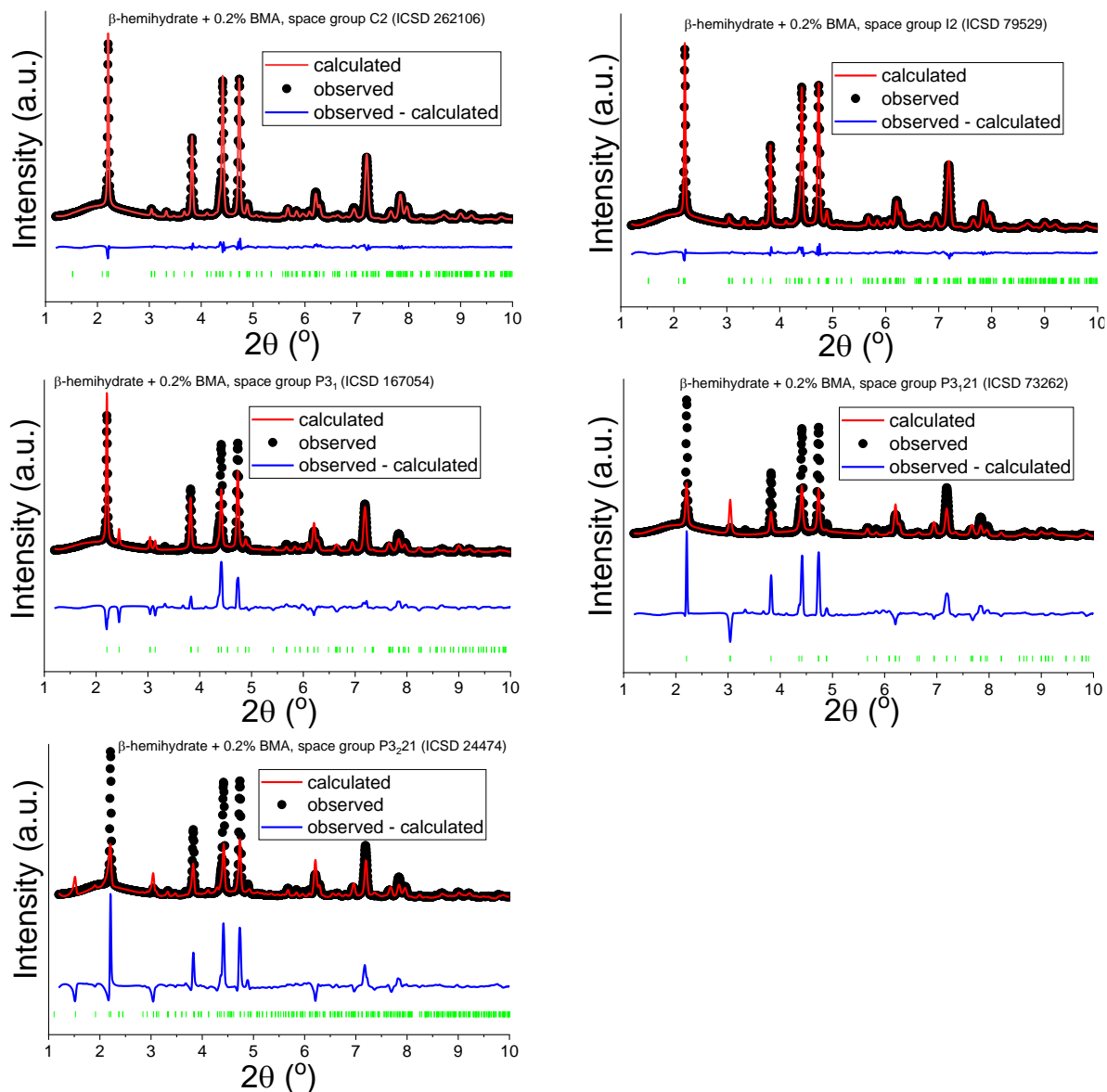


**Figure S14** The results of structural refinements with the different models reported in the ICSD for  $\beta\text{-CaSO}_4\cdot 0.5\text{H}_2\text{O}$  with 0.2 % w/w BMA.

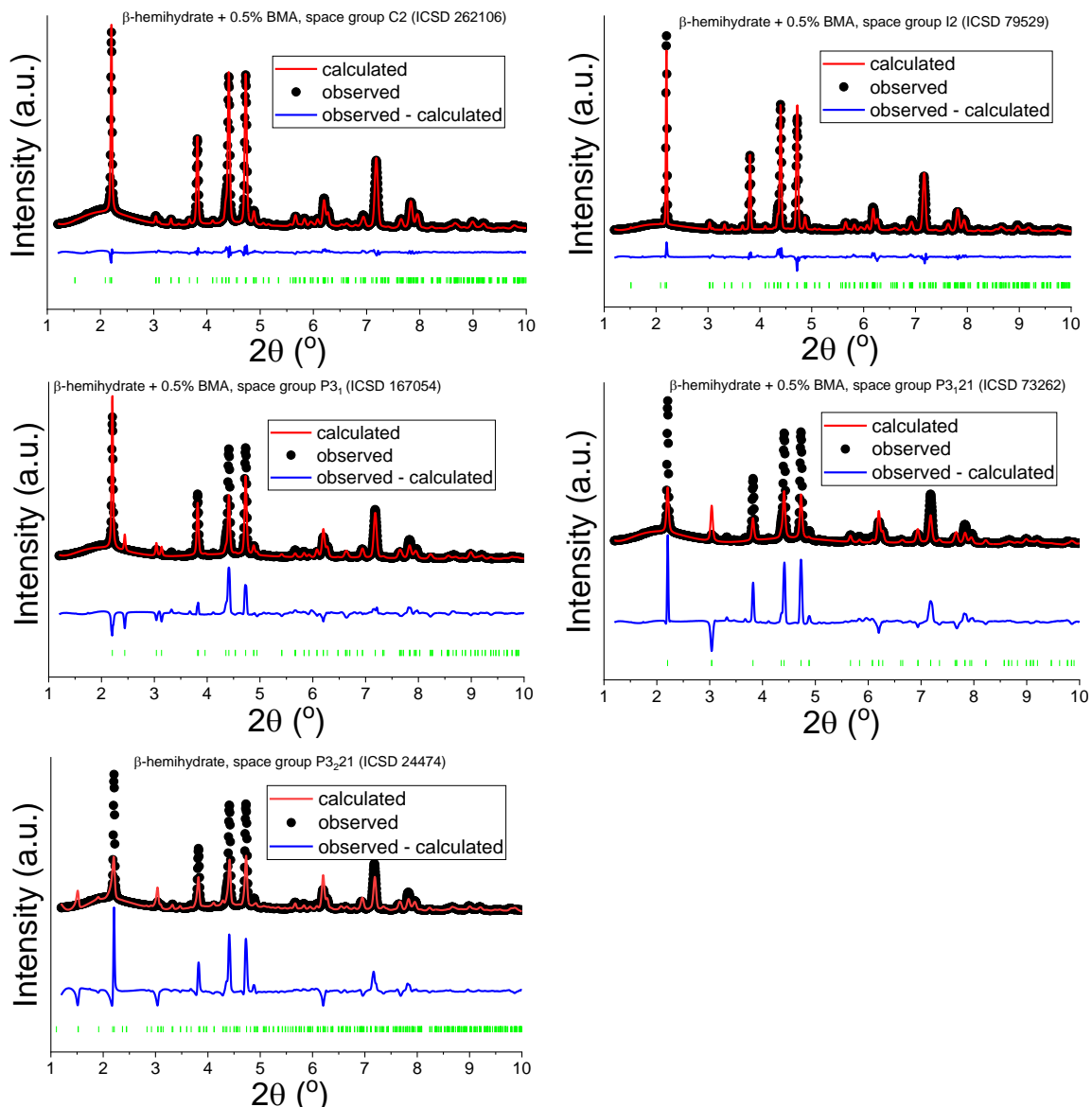


**Figure S15** The results of structural refinements with the different models reported in the ICSD for  $\beta\text{-CaSO}_4\cdot 0.5\text{H}_2\text{O}$  with 0.5 % w/w BMA.

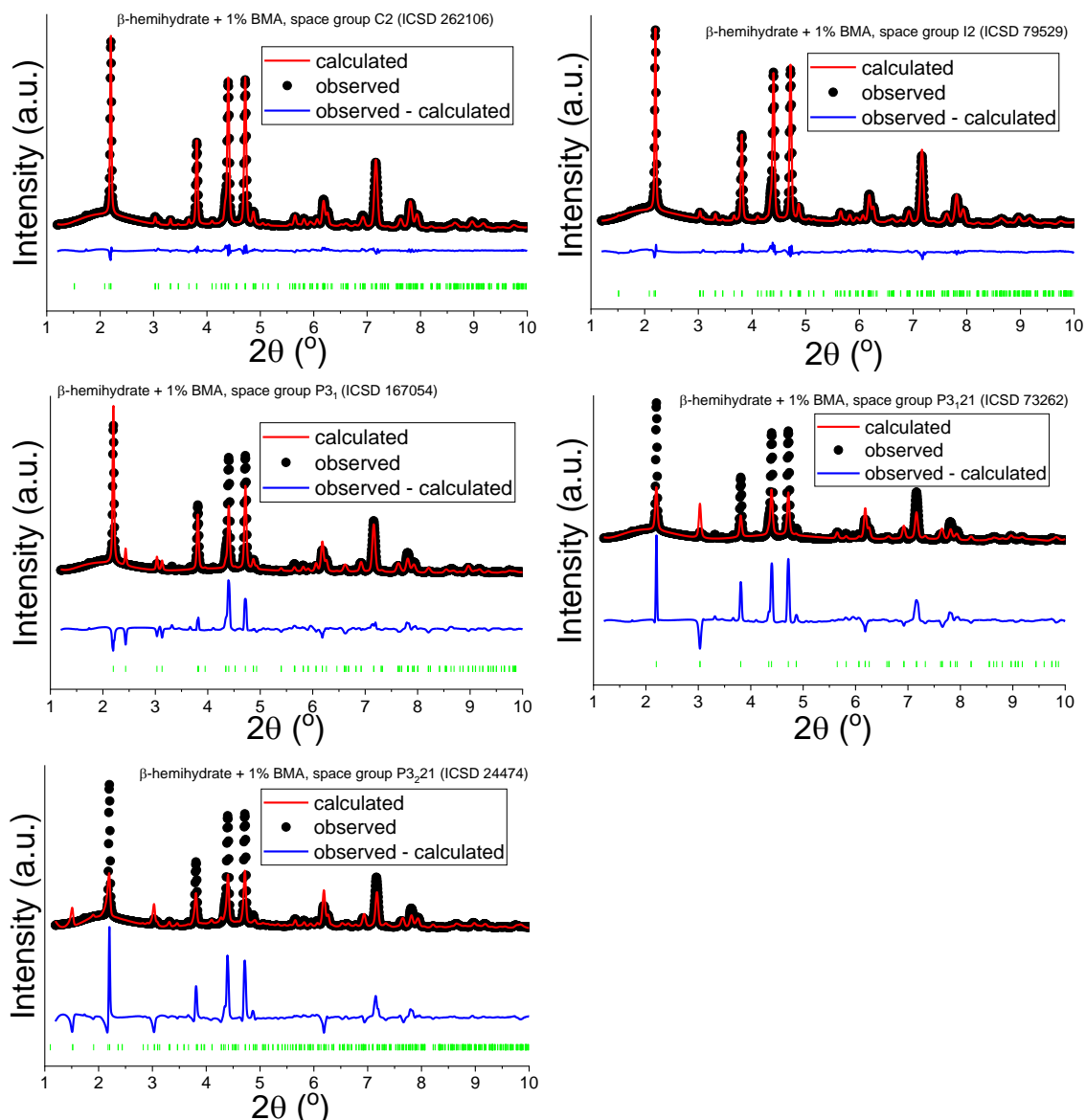


**Figure S16** The results of structural refinements with the different models reported in the ICSD for  $\beta\text{-CaSO}_4\cdot 0.5\text{H}_2\text{O}$  with 1 % w/w BMA.

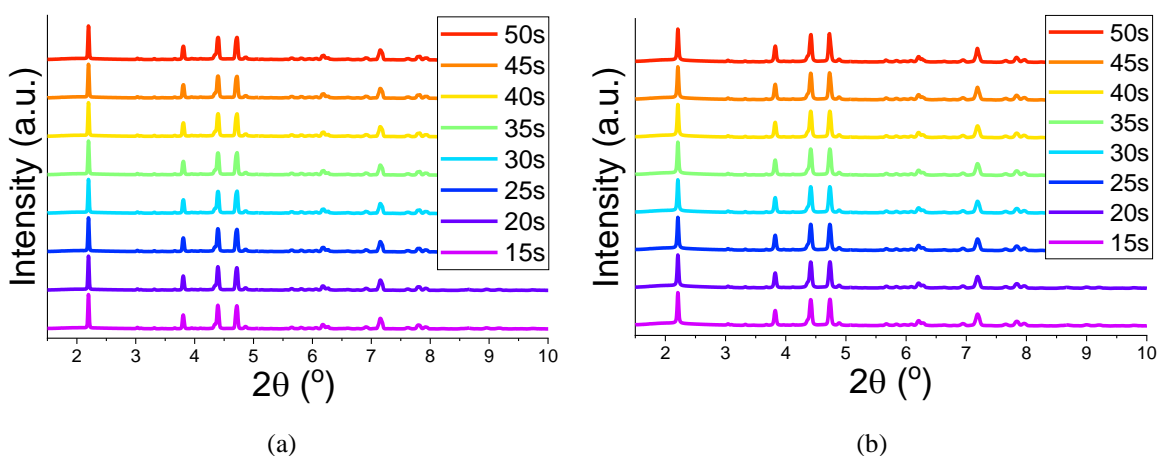


**Figure S17** The XRD patterns recorded at the synchrotron (a) for  $\alpha$ -hemihydrate, water added after 25s; (b) for  $\beta$ -hemihydrate, water added after 20s.

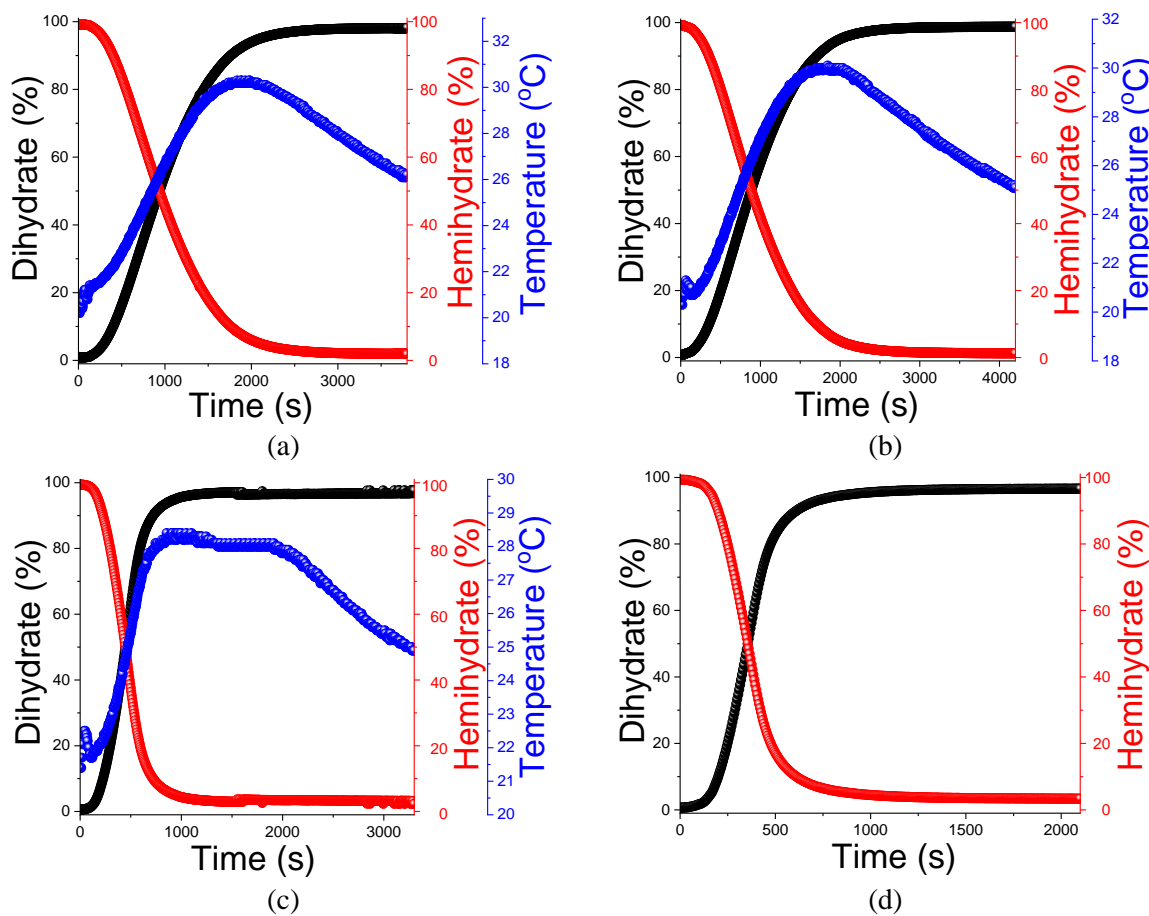


**Figure S18** In situ data showing the hydration of (a)  $\alpha\text{-CaSO}_4\cdot0.5\text{H}_2\text{O} + 0.2\%$  BMA; (b)  $\alpha\text{-CaSO}_4\cdot0.5\text{H}_2\text{O} + 0.5\%$  BMA; (c)  $\beta\text{-CaSO}_4\cdot0.5\text{H}_2\text{O} + 0.2\%$  BMA; (d)  $\beta\text{-CaSO}_4\cdot0.5\text{H}_2\text{O} + 0.5\%$  BMA (a fault with the probe meant that no accurate temperature data were recorded for his reaction). Phase fractions of the hemi- and dihydrate were determined by batch Rietveld refinements, and are plotted in percentage terms.

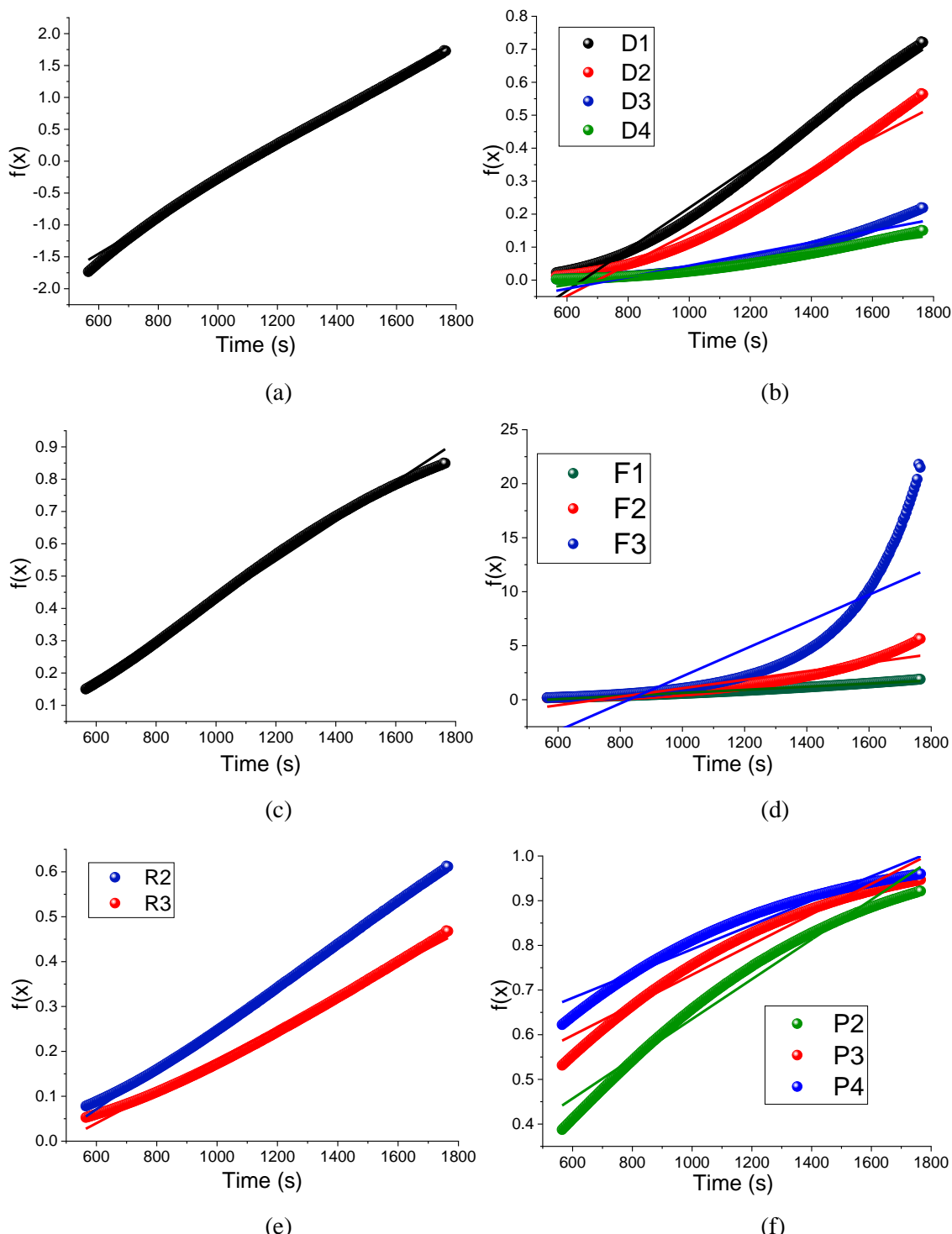


**Figure S19** Fits of selected kinetic models to the hydration of  $\alpha\text{-CaSO}_4\cdot0.5\text{H}_2\text{O}$ , showing the (a) Prout-Tompkins; (b) diffusion; (c) zero-order; (d) first-, second- and third-order; (e) R2 contracting area and R3 contracting volume; and, (f) power law models.

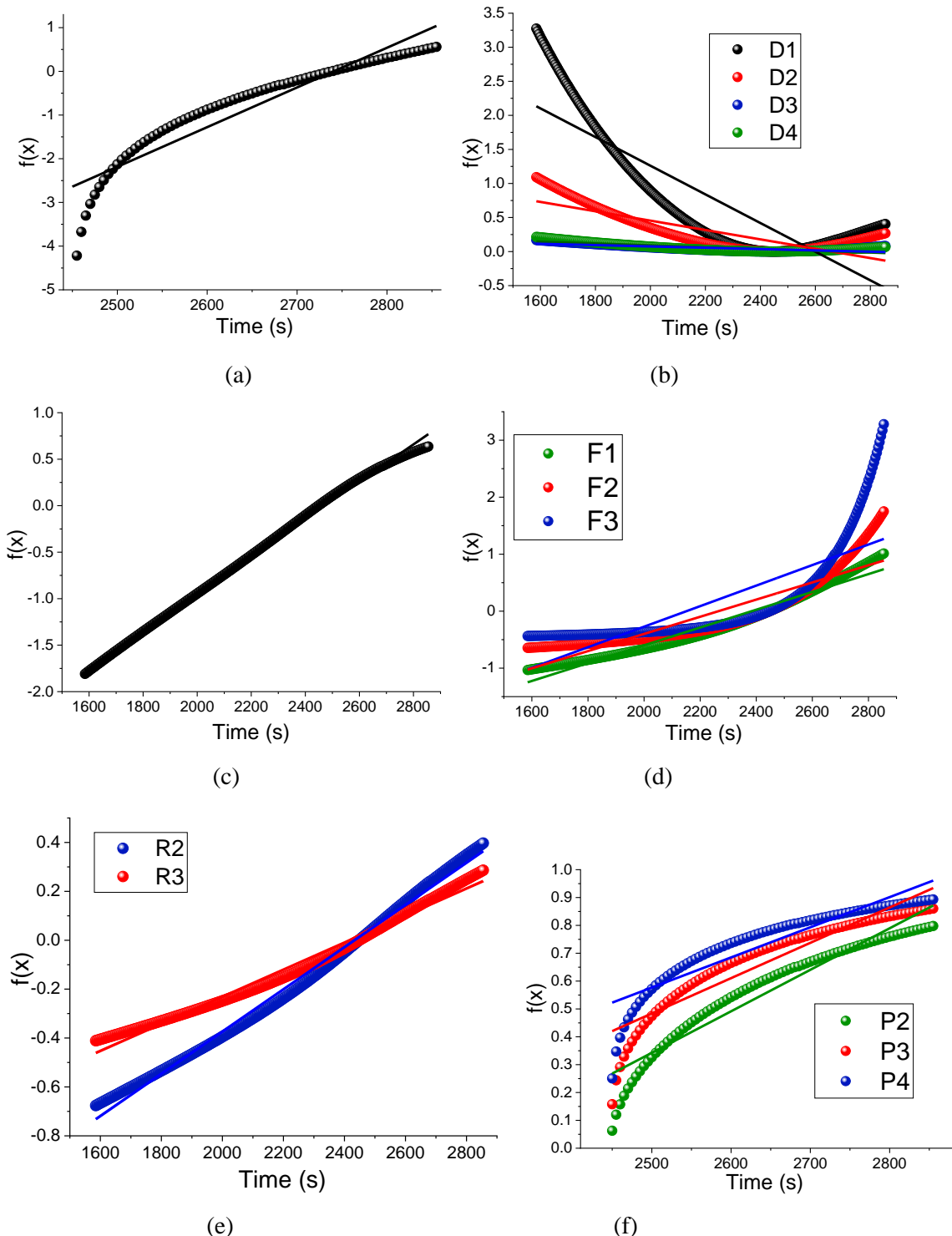


**Figure S20** Fits of selected kinetic models to the hydration of  $\beta\text{-CaSO}_4 \cdot 0.5\text{H}_2\text{O}$ , showing the (a) Prout-Tompkins; (b) diffusion; (c) zero-order; (d) first-, second- and third-order; (e) R2 contracting area and R3 contracting volume; and, (f) power law models.

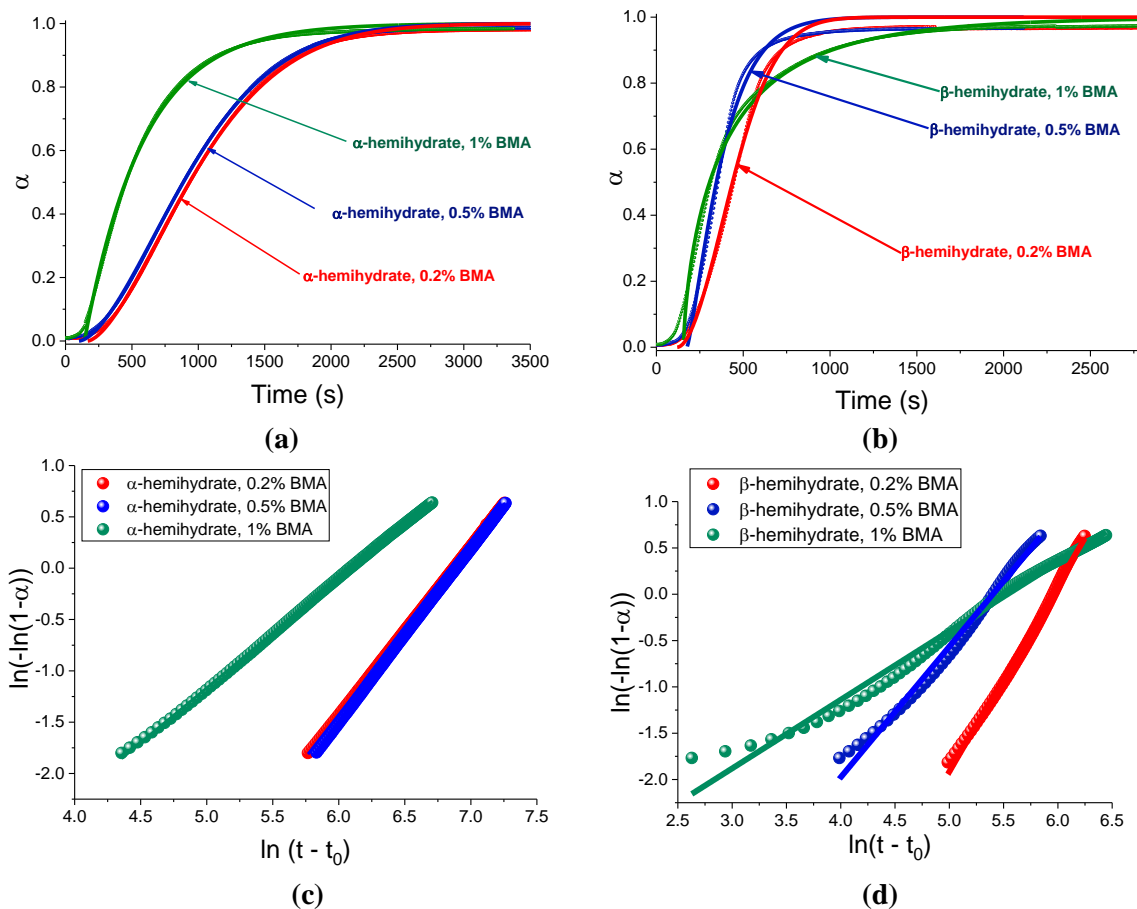


**Figure S21** Avrami-Erofe'ev fitting to accelerated hydration reactions, showing direct fits to the experimental data for (a)  $\alpha$ -CaSO<sub>4</sub>·0.5H<sub>2</sub>O and (b)  $\beta$ -CaSO<sub>4</sub>·0.5H<sub>2</sub>O and Sharp-Hancock plots for (c)  $\alpha$ -CaSO<sub>4</sub>·0.5H<sub>2</sub>O and (d)  $\beta$ -CaSO<sub>4</sub>·0.5H<sub>2</sub>O.

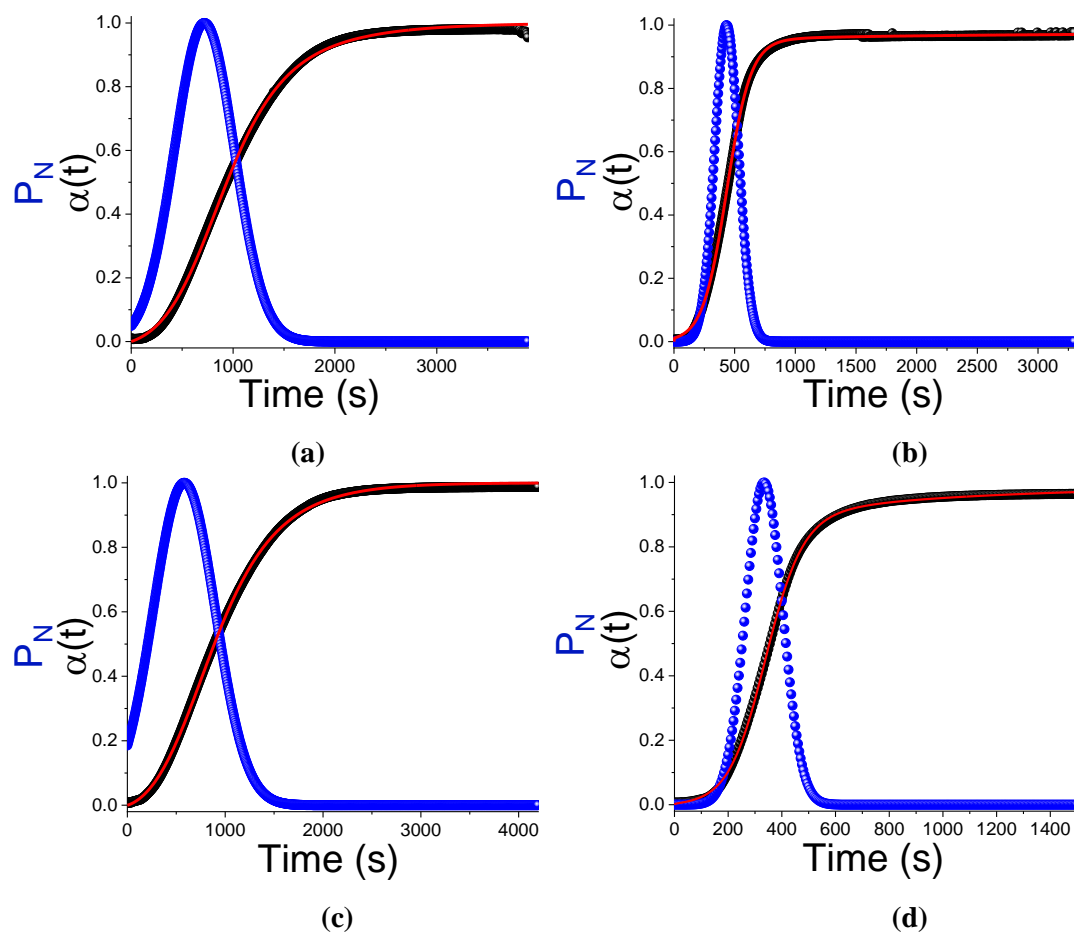


**Figure S22** Gaultieri fits for the hydration of (a)  $\alpha\text{-CaSO}_4\cdot0.5\text{H}_2\text{O}$  with 0.2 % w/w BMA; (b)  $\beta\text{-CaSO}_4\cdot0.5\text{H}_2\text{O}$  with 0.2 % w/w BMA; (c)  $\alpha\text{-CaSO}_4\cdot0.5\text{H}_2\text{O}$  with 0.5 % w/w BMA; and, (d)  $\beta\text{-CaSO}_4\cdot0.5\text{H}_2\text{O}$  with 0.5 % w/w BMA. Experimental data (■), corresponding Gaultieri fits (—) and the calculated rate of nucleation ( $P_N$ ; ●) are depicted.

**Table S1** Refinement data for  $\alpha$ - and  $\beta$ -CaSO<sub>4</sub>·0.5H<sub>2</sub>O.

Space group	$\alpha$ -hemihydrate					
	a (Å)	b (Å)	c (Å)	$\alpha$ (°)	$\beta$ (°)	$\gamma$ (°)
<i>C2</i> ICSD 262106	17.379(2)	6.904(1)	11.992(1)	90	133.421(7)	90
<i>I2</i> ICSD 79529	11.942(1)	6.869(1)	12.569(0)	90	90.221(2)	90
<i>P3<sub>1</sub></i> ICSD 167054	6.917(2)	6.914(1)	12.623(2)	90	90	120
<i>P3<sub>2</sub>1</i> ISCD 24474	13.83(2)	13.800(2)	12.596(4)	90	90	120.1(1)
<i>P3<sub>1</sub>21</i> ICSD 73262	6.910(1)	6.918(9)	6.313(3)	90	90	120.0(1)

Space group	$\beta$ -hemihydrate					
	a (Å)	b (Å)	c (Å)	$\alpha$ (°)	$\beta$ (°)	$\gamma$ (°)
<i>C2</i> ICSD 262106	17.342(3)	6.889(0)	11.908(1)	90	133.546(9)	90
<i>I2</i> ICSD 79529	11.942(1)	6.869(1)	12.570(0)	90	90.21(1)	90
<i>P3<sub>1</sub></i> ICSD 167054	6.885(2)	6.882(1)	12.569(2)	90	90	120
<i>P3<sub>2</sub>1</i> ISCD 24474	13.760(2)	13.730(1)	12.542(4)	90	90	120.07(9)
<i>P3<sub>1</sub>21</i> ICSD 73262	6.880(1)	6.889(9)	6.285(2)	90	90	120.0(1)

**Table S2**  $R_{wp}$  factors for  $\alpha$ - and  $\beta$ -CaSO<sub>4</sub>·0.5H<sub>2</sub>O, with and without the presence of BMA.

Sample	Space group				
	C2 ICSD 262106	I2 ICSD 79529	P3 <sub>1</sub> ICSD 167054	P3 <sub>1</sub> 21 ICSD 24474	P3 <sub>1</sub> 21 ICSD 73262
$\alpha$ -CaSO <sub>4</sub> ·0.5H <sub>2</sub> O	4.737	7.660	20.146	35.400	36.640
$\alpha$ -CaSO <sub>4</sub> ·0.5H <sub>2</sub> O + 0.2 % BMA	4.017	13.047	21.852	33.027	34.058
$\alpha$ -CaSO <sub>4</sub> ·0.5H <sub>2</sub> O + 0.5 % BMA	4.626	4.735	19.196	34.608	31.382
$\alpha$ -CaSO <sub>4</sub> ·0.5H <sub>2</sub> O + 1 % BMA	4.750	4.750	20.070	31.002	32.699
$\beta$ -CaSO <sub>4</sub> ·0.5H <sub>2</sub> O	3.868	4.581	25.444	39.949	40.311
$\beta$ -CaSO <sub>4</sub> ·0.5H <sub>2</sub> O + 0.2 % BMA	7.387	6.599	21.841	35.095	35.512
$\beta$ -CaSO <sub>4</sub> ·0.5H <sub>2</sub> O + 0.5 % BMA	7.712	7.211	25.534	39.387	39.712
$\beta$ -CaSO <sub>4</sub> ·0.5H <sub>2</sub> O + 1 % BMA	7.565	7.957	24.826	39.223	39.886

**Table S3** Refinement data for  $\alpha$ - and  $\beta$ -dihydrate.

Space group	$\alpha$ -dihydrate					
	a (Å)	b (Å)	c (Å)	$\alpha$ (°)	$\beta$ (°)	$\gamma$ (°)
<i>C2/c</i> <b>ICSD 15982</b>	6.260(2)	15.154(7)	5.656(2)	90	114.13(4)	90
$\beta$ -dihydrate						
<i>C2/c</i> <b>ICSD 15982</b>	6.2485(2)	15.117(9)	5.645(2)	90	114.13(5)	90

**Table S4** The full list of kinetic models explored.

Kinetic model	Description	Function
AE	Avrami-Erofe'ev	$1 - e^{-k(t-t_0)^n}$
B1	Prout-Tompkins	$[-\ln(1 - \alpha)] + c^a$
D1	1-D diffusion	$\alpha^2$
D2	2-D diffusion	$((1 - \alpha)\ln(1 - \alpha)) + \alpha$
D3	3-D diffusion-Jander	$(1 - (1 - \alpha)^{1/3})^2$
D4	Ginstling-Brounshtein	$1 - (2/3)\alpha - (1 - \alpha)^{2/3}$
F0/R1	Zero-order	$\alpha$
F1	First-order	$-\ln(1 - \alpha)$
F2	Second-order	$[1/(1 - \alpha)] - 1$
F3	Third-order	$(1/2)[(1 - \alpha)^2 - 1]$
R2	Contracting area	$1 - (1 - \alpha)^{1/2}$
R3	Contracting volume	$1 - (1 - \alpha)^{1/3}$
P2	Power law	$\alpha^{1/2}$
P3	Power law	$\alpha^{1/3}$
P4	Power law	$\alpha^{1/4}$

**Table S5** R<sup>2</sup> fitting values obtained when applying the full set of kinetic models for the hydration of α- and β-CaSO<sub>4</sub>·0.5H<sub>2</sub>O.

Kinetic model	α	α + 0.2% BMA	α + 0.5% BMA	α + 1% BMA	β	β + 0.2% BMA	β + 0.5% BMA	β + 1% BMA
A2	0.9999	0.9991	0.9793	0.9729	0.9688	0.9676	0.9579	0.9490
A3	0.9976	0.9938	0.9397	0.9394	0.9297	0.9283	0.9203	0.9034
A4	0.9944	0.9891	0.9072	0.9159	0.9016	0.9007	0.8957	0.8724
B1	0.9964	0.9924	0.7907	0.8644	0.8284	0.8348	0.8478	0.8000
D1	0.9863	0.9927	0.5064	0.3444	0.7161	0.6236	0.5387	0.2235
D2	0.9653	0.9769	0.4430	0.2513	0.6720	0.5701	0.4599	0.1180
D3	0.9241	0.9416	0.2939	0.0927	0.5409	0.6236	0.2809	0.0064
D4	0.9530	0.9668	0.4043	0.2036	0.6409	0.5343	0.4131	0.0746
F0/R1	0.9946	0.9894	0.9667	0.9218	0.9977	0.9896	0.9737	0.8403
F1	0.9796	0.9876	0.9923	0.9986	0.9579	0.9772	0.9922	0.9764
F2	0.8766	0.8969	0.8821	0.9364	0.8094	0.8449	0.8947	0.9861
F3	0.7267	0.7565	0.7052	0.7922	0.6283	0.6700	0.7434	0.8931
P2	0.9737	0.9624	0.9409	0.9287	0.9220	0.9204	0.9057	0.8906
P3	0.9620	0.9488	0.8877	0.8863	0.8732	0.8721	0.8616	0.8364
P4	0.9553	0.9411	0.8495	0.8599	0.8416	0.8416	0.8351	0.8025
R2	0.9982	0.9996	0.996	0.9762	0.9926	0.9993	0.9976	0.9205
R3	0.9946	0.9983	0.9988	0.9877	0.9845	0.9956	0.9993	0.9425
Gualtieri	0.9994	0.9992	0.9995	0.9989	0.9992	0.9996	0.9998	0.9991